

Degradation and its fast recovery in a-IGZO thin-film transistors under negative gate bias stress

Jianing Guo(郭佳宁), Dongli Zhang(张冬利), Mingxiang Wang(王明湘), and Huaisheng Wang(王槐生)
Citation: Chin. Phys. B, 2021, 30 (**11**): 118102. DOI: 10.1088/1674-1056/ac05aa
Journal homepage: http://cpb.iphy.ac.cn; http://iopscience.iop.org/cpb

What follows is a list of articles you may be interested in

Synaptic plasticity and classical conditioning mimicked in single indium-tungsten-oxide based neuromorphic transistor

Rui Liu(刘锐), Yongli He(何勇礼), Shanshan Jiang(姜珊珊), Li Zhu(朱力), Chunsheng Chen(陈春生), Ying Zhu(祝影), and Qing Wan(万青)
Chin. Phys. B, 2021, 30 (**5**): 058102. DOI: 10.1088/1674-1056/abc163

Enhanced mobility of MoS_2 field-effect transistors by combining defect passivation with dielectric-screening effect

Zhao Li(李钊), Jing-Ping Xu(徐静平), Lu Liu(刘璐), and Xin-Yuan Zhao(赵心愿)
Chin. Phys. B, 2021, 30 (**1**): 018102. DOI: 10.1088/1674-1056/abb30f

A systematic study of light dependency of persistent photoconductivity in a-InGaZnO thin-film transistors

Yalan Wang(王雅兰), Mingxiang Wang(王明湘), Dongli Zhang(张冬利), and Huaisheng Wang(王槐生)
Chin. Phys. B, 2020, 29 (**11**): 118101. DOI: 10.1088/1674-1056/abb222

Improved performance of back-gate MoS_2 transistors by NH_3-plasma treating high-*k* gate dielectrics

Jian-Ying Chen(陈建颖), Xin-Yuan Zhao(赵心愿), Lu Liu(刘璐), Jing-Ping Xu(徐静平)
Chin. Phys. B, 2019, 28 (**12**): 128101. DOI: 10.1088/1674-1056/ab50fe

Electronic transport properties of silicon junctionless nanowire transistors fabricated by femtosecond laser direct writing

Liu-Hong Ma(马刘红), Wei-Hua Han(韩伟华), Hao Wang(王昊), Qi-feng Lyu(吕奇峰), Wang Zhang(张望), Xiang Yang(杨香), Fu-Hua Yang(杨富华)
Chin. Phys. B, 2016, 25 (**6**): 068103. DOI: 10.1088/1674-1056/25/6/068103

Degradation and its fast recovery in a-IGZO thin-film transistors under negative gate bias stress*

Jianing Guo(郭佳宁), Dongli Zhang(张冬利)†, Mingxiang Wang(王明湘), and Huaisheng Wang(王槐生)

School of Electronic and Information Engineering, Soochow University, Suzhou 215006, *China*

(Received 1 April 2021; revised manuscript received 18 May 2021; accepted manuscript online 27 May 2021)

A new type of degradation phenomena featured with increased subthreshold swing and threshold voltage after negative gate bias stress (NBS) is observed for amorphous InGaZnO (a-IGZO) thin-film transistors (TFTs), which can recover in a short time. After comparing with the degradation phenomena under negative bias illumination stress (NBIS), positive bias stress (PBS), and positive bias illumination stress (PBIS), degradation mechanisms under NBS is proposed to be the generation of singly charged oxygen vacancies (V_o^+) in addition to the commonly reported doubly charged oxygen vacancies (V_o^{2+}). Furthermore, the NBS degradation phenomena can only be observed when the transfer curves after NBS are measured from the negative gate bias to the positive gate bias direction due to the fast recovery of V_o^+ under positive gate bias. The proposed degradation mechanisms are verified by TCAD simulation.

Keywords: amorphous IGZO, thin-film transistors, negative bias stress, subthreshold swing

PACS: 81.05.Gc, 81.05.Ea, 85.30.Tv **DOI:** 10.1088/1674-1056/ac05aa

1. Introduction

Amorphous InGaZnO (a-IGZO) thin-film transistors (TFTs) have attracted much attention due to the characteristics including high electron mobility, low leakage current, small subthreshold swing, and high large-area uniformity. a-IGZO TFTs with a back-channel etching (BCE) structure have no protection at the back channel. Thus, the back channel may be damaged during the patterning of the source/drain electrodes, and the device performance becomes deteriorated.[1] In the etching-stop layer (ESL) structure, a dielectric layer is deposited to protect the back channel. However, an extra mask is required to pattern the ESL, which increases the process complexity. The ESL also increases the characteristic size of the device. Elevated-metal metal–oxide (EMMO) TFT makes up for the shortcomings of traditional BCE and ESL TFTs by elevating the source/drain electrodes above the passivation layer and the formation of conductive source/drain regions.[2,3]

For the a-IGZO TFTs in the pixel and driver circuits of active-matrix display panels, understanding the degradation mechanisms under various types of bias stresses is greatly important for the optimization of device structure and fabrication process. The most frequently concerned stress conditions include positive gate bias stress (PBS), negative bias stress (NBS), negative bias illumination stress (NBIS), and positive bias illumination stress (PBIS). In the previous work on PBS, the common degradation phenomenon is the positive shift of transfer curve. It is explained with electron trapping in the gate dielectric or at the interface between the channel and the gate dielectric.[4] However, for PBIS, the transfer curve also shifts to the positive gate bias direction but the shift is less than that under PBS because the ionized oxygen vacancies (V_o^{2+}) generated with the help of light move to the back channel and contribute a negative shift of the transfer curve.[5,6] The transfer curve of a-IGZO TFTs generally shifts to the negative gate bias direction under NBS due to the generation and accumulation of V_o^{2+} at the interface between the channel and the gate insulator.[7–10] The negative shift of the transfer curve under NBIS is more evident, where the mechanism is similar to that under NBS, but the density of V_o^{2+} is larger with the help of illumination.[8,11]

In this paper, positive shift of the transfer curve and severe degradation in the subthreshold characteristics were observed for a-IGZO TFTs under NBS and NBIS, and a gentle degradation is observed under PBS and PBIS. A fast recovery of the degradation in the threshold voltage (V_{TH}) and subthreshold swing (SS) is observed for the a-IGZO TFTs under NBS and NBIS, and no degradation can be observed when the transfer curves are measured with gate bias sweeping from positive gate bias to negative gate bias direction. The mechanisms for the degradation and its recovery under gate bias stress with or without illuminations are proposed.

2. Experiments

As shown in Fig. 1, the a-IGZO TFTs with an EMMO structure were fabricated and used. A 300-nm thick Mo was

*Project supported in part by the National Natural Science Foundation of China (Grant Nos. 61971299 and 61974101), the Natural Science Foundation of Jiangsu Province, China (Grant No. SBK2020021406), the Fund from the State Key Laboratory of ASIC and System, Fudan University (Grant No. 2019KF007), the Fund from the Suzhou Science and Technology Bureau (Grant No. SYG201933), and the Fund from the Jiangsu Higher Education Institute of China (Grant No. 19KJB510058).

†Corresponding author. E-mail: dongli_zhang@suda.edu.cn

© 2021 Chinese Physical Society and IOP Publishing Ltd

sputtered and patterned as the gate electrode. The gate insulator consists of 50-nm silicon nitride (SiN_x) and 75-nm silicon dioxide (SiO_x), deposited by plasma-enhanced chemical vapor deposition (PECVD). A two-hour annealing at 400 °C was performed in O_2 to remove the residual hydrogen in the gate insulator. Then, a 20-nm a-IGZO was sputtered at room temperature as the active layer. The passivation layer is 300-nm SiO_x deposited by PECVD, and another dehydrogenation treatment was performed in O_2 for two hours. After metallization, a critical oxidizing heat treatment was performed at 400 °C for two hours to form the low-resistance source/drain regions.

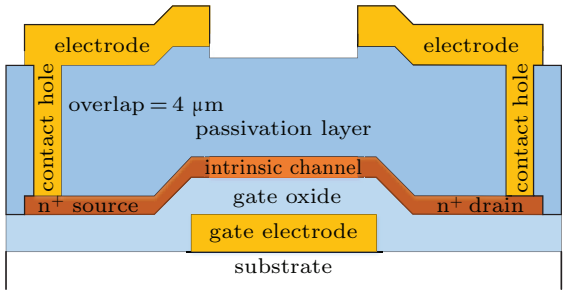


Fig. 1. Schematic cross-sectional diagram of the EMMO-type a-IGZO TFT.

For the reliability experiments under gate bias stress, the source/drain electrodes were grounded and the gate electrodes was applied with a bias of −20 V or 20 V. Illumination is applied with LED monochromatic light sources with wavelengths of 660 nm (red), 520 nm (green), and 445 nm (blue). The transfer curves of the TFTs before and after stress were measured with Agilent 4156C semiconductor parameter analyzer, and the transfer curves before and after NBIS and PBIS were measured under illumination. The channel width and length of a-IGZO TFTs are 50 μm and 20 μm, respectively, and the overlap between the gate and source/drain electrodes is 4 μm. V_{TH} is estimated by the linear extrapolation method from the transfer curve at V_{ds} of 0.1 V. The flat-band voltage (V_{FB}) is defined as the gate voltage at which drain current begins to transit to the subthreshold region.

3. Results and discussion

3.1. NBS and NBIS degradation

As shown in Fig. 2(a), the transfer curve shows an evident degradation in the subthreshold swing and threshold voltage after NBS with a gate voltage of −20 V. The variations of V_{TH} (ΔV_{TH}) and *SS* (ΔSS) are extracted and plotted *versus* stress time in Fig. 3. V_{TH}, V_{FB}, and *SS* behave differently with stress time, where V_{TH} initially exhibits an evident positive shift after 10 s and continues to gradually shift toward positive gate bias direction with the increase in stress time, *SS* increases significantly after 10-s stress time, but it remains almost unchanged during the following stress period. However, V_{FB} increases continually with the increase in stress time. This rapid degradation of V_{TH} has also been observed in previous studies, where the V_{TH} shifts toward negative gate bias direction rather than positive gate bias direction.[12] The degradations in V_{TH}, V_{FB}, and *SS* can be recovered, but the corresponding recovery also behaves differently. One can notice from Fig. 2(b) that the degradation in *SS* recovers fast in the first 10 s after the stress is removed and gradually recovers completely in 1800 s. V_{FB} recovers completely in 10 s but V_{TH} recovers more slowly.

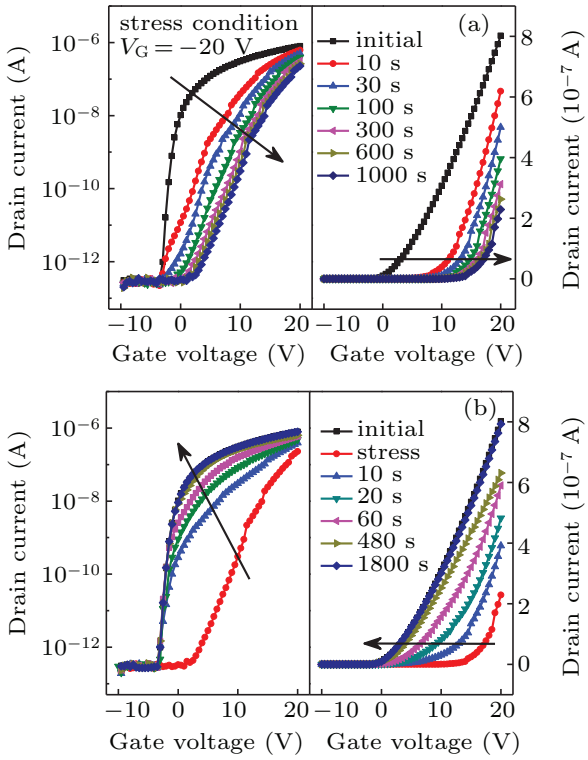


Fig. 2. Evolutions of the transfer curves in linear and logarithmic scales for the TFTs (a) under NBS and (b) after NBS is removed.

For a-IGZO TFTs under NBS, the transfer curve is generally observed to shift toward the negative gate bias direction due to the generation of V_o^{2+}, which acts as shallow donor states and distribute near the conduction band. However, the observed positive shift of the transfer curve after NBS indicates that other degradation mechanisms are involved in addition to the generation of V_o^{2+}. Increased *SS* implies an increase in deep states in the bandgap. The density of increased deep states (ΔD_{ds}) is extracted approximately 5.17×10^{12} cm$^{-2}\cdot$eV^{-1} with the following relationship:

$$\Delta D_{ds} = \frac{C_{ox}}{q}\frac{\Delta SS}{k_B T\,(\ln 10)}, \tag{1}$$

where C_{ox} is the oxide capacitance per unit area, q is the elementary charge, k_B is the Boltzmann constant, and T is the absolute temperature. In a-IGZO, singly charged oxygen vacancies (V_o^+) are the main type of deep states,[13] which is a metastable state and can explain the fast recovery of the *SS* after stress. The increased deep states can also trap parts of the accumulated carriers and increase the threshold voltage.

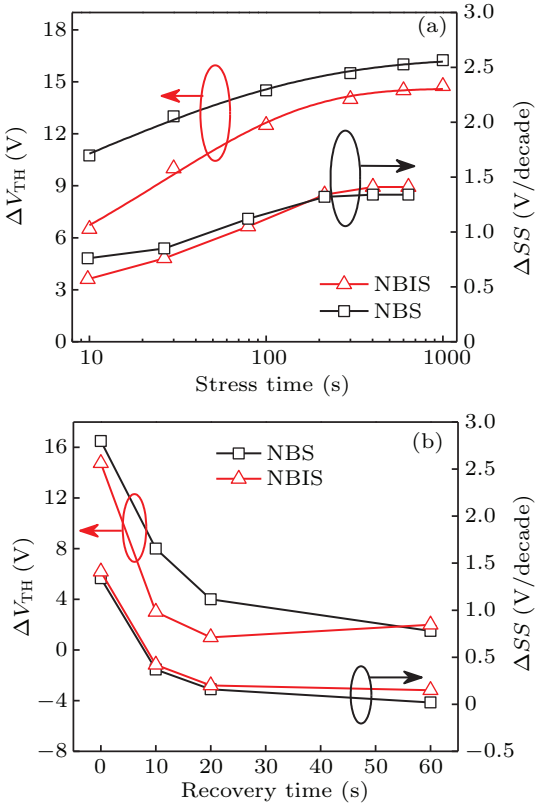


Fig. 3. (a) ΔV_{TH} and ΔSS under NBS and NBIS with the stress time and (b) with the recovery time after the stress is removed.

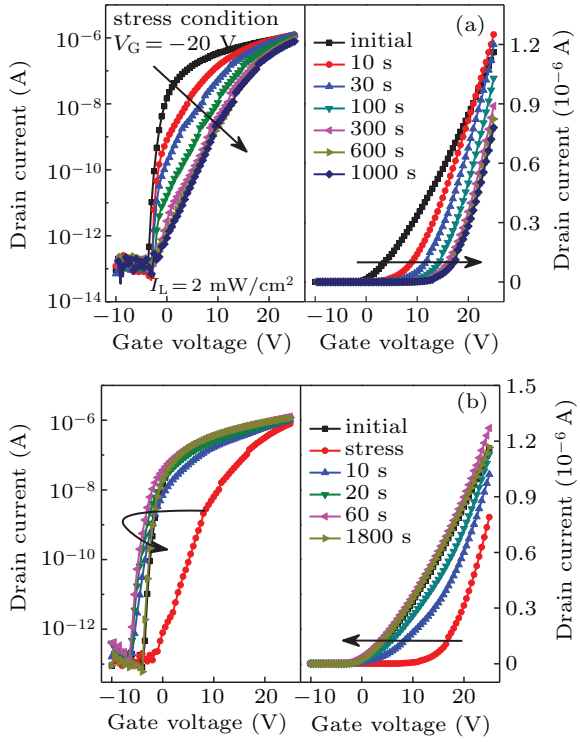


Fig. 4. Evolution of the transfer curves in linear and logarithmic scales for the TFTs (a) under NBIS and (b) after NBIS is removed.

Figure 4(a) shows that the degradation phenomena of NBIS with blue light of a power density (I_L) of 2 mW/cm^2 are similar to those under NBS, *i.e.*, *SS* and V_{TH} are increased. The slope of transfer curve in on-state is also increased. But differently, no evident positive shift of V_{FB} is found under NBIS. Furthermore, as shown in Fig. 4(b), V_{FB} initially exhibits a negative shift and then recovers to its initial values after the NBIS is removed. For the first time such type of recovery phenomenon has been reported.

NBIS usually introduces more severe degradation than NBS due to the ionization of neutral oxygen vacancies under illumination.[9,13] However, after comparing the degradation and recovery of *SS* and V_{TH} under NBS and NBIS, as shown in Fig. 3, the shift of V_{TH} under NBIS is found to be smaller than that under NBS. Thus, two degradation mechanisms involved under NBIS are proposed. One mechanism is caused by the negative gate bias, and the corresponding degradation is similar to that under NBS. The features include increase in *SS*, V_{TH}, and V_{FB} and their recovery in a short time. The other mechanism causes negative shift in V_{FB} and V_{TH}, resulting in the smaller shift of V_{FB} and V_{TH} under NBIS than that under NBS. Moreover, the a-IGZO TFT after NBIS shows a negative shift of V_{FB} after the rapid recovery of the on-state characteristics.

The dependence of ΔV_{TH} on stress time after NBS and NBIS was fitted with the stretched exponential function, as follows:

$$\Delta V_{TH} = \Delta V_{TH}(0)\left\{1-\exp\left[-\left(\frac{t}{\tau}\right)^{\beta}\right]\right\}, \quad (2)$$

where $\Delta V_{TH}(0)$ is the saturation value of ΔV_{TH} at an infinite time, τ is a characteristic time, and β is the stretched-exponential exponent. The fitting results are summarized in Table 1, where the prefactor $\Delta V_{TH}(0)$ is 16.4 V, τ is 7.6 s, and β is 0.31. The degradations dominated by the generation of V_o^{2+} can also be described with the stretched exponential function,[14] but its effect on V_{TH} is opposite to that of V_o^{+}. Thus, it is within expectation that the τ for NBIS is larger than that of NBS, as shown in Table 1.

Table 1. Fitting parameters for the fitting of the dependence of ΔV_{TH} on stress time after NBS and NBIS with the stretched exponential function.

Parameters	Value	
	NBS	NBIS
$\Delta V_{TH}(0)$ (V)	16.35	14.61
τ (s)	7.56	25.73
β	0.31	0.51

To clarify the degradation mechanism, which causes the negative shift of V_{FB} after the removal of NBIS, the degradation of a-IGZO TFT under illumination stress only was further investigated. As shown in Fig. 5, under the illumination of blue light with a power density of 2 mW/cm^2, only a small amount of increase in the on-state current (I_{on}) is found, and the increase in I_{on} does not increase with the increase in stress time. Thus, the increase in I_{on} under illumination is proposed due to the photo generated carriers.[15] Then, the negative shift of V_{FB} after NBIS should be caused by the combination of the

negative gate voltage and illumination. It is speculated that the negative shift of V_{FB} observed during the recovery of NBIS degradation is caused by V_o^{2+} similar to that in conventional NBS experiments.[7–9] A large number of V_o^{2+} is generated under NBIS; thus, a smaller positive shift of V_{FB} under NBIS than that under NBS is reasonable. After the fast recovery of V_o^{+} after NBIS removal that results into the positive shift of V_{FB}, the generated V_o^{2+} dominates the performance of TFT, which exhibits a negative shift of V_{FB}.

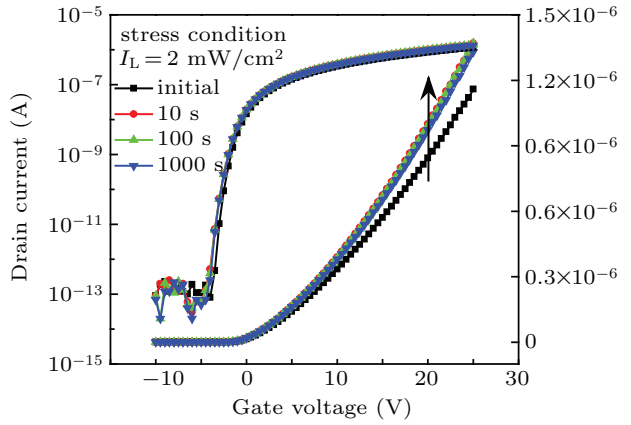


Fig. 5. Evolution of the transfer curves in linear and logarithmic scales for the TFTs under illumination with blue light.

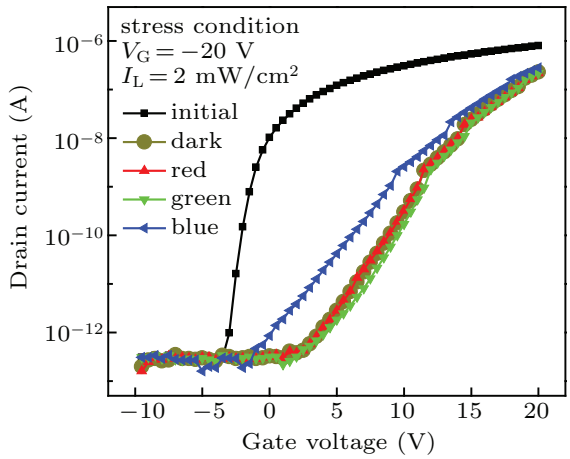


Fig. 6. Comparison of the transfer curves of the a-IGZO TFTs before and after NBIS with the light of different wavelengths.

To confirm this hypothesis, experiments were carried out under the same gate bias and light power density but illuminated with lights of different wavelengths. Figure 6 shows that the degradation under NBIS with red light is the same as that under NBS, indicating that red light does not contribute to the NBS degradation. Under green light illumination, the degradation under NBIS is also almost the same as the one under NBS. While when the illumination is performed with blue light during NBIS, V_{FB} shows a smaller positive shift and *SS* increases. The photon energy for the red, green, and blue light is 1.9, 2.4, and 2.8 eV, respectively. V_o^{2+} and V_o^{+} would form trap states above the valence band maximum with an energy difference up to 2.9 eV and 2.6 eV, respectively.[16] Thus, the energy of red light is too small for the ionization of neutral oxygen vacancies. Under green light, the energy is insufficient to generate V_o^{+}, either. Under blue light, V_o^{+} and V_o^{2+} can be produced by the ionization of neutral oxygen vacancies (V_o). Therefore, compared with that under NBS, the positive shift of V_{FB} becomes smaller due to the increase in V_o^{2+}, and the increase in ΔSS is due to more V_o^{+} generated.

3.2. PBS and PBIS degradation

Degradation of the a-IGZO TFTs under PBS was also investigated to further understand the degradation mechanism when V_o^{+} and V_o^{2+} were involved. As shown in Fig. 7(a), under a gate voltage of 20 V, the transfer curve shows a negative shift as small as 0.95 V. Electron trapping in the gate oxide may also occur during PBS, but it results into positive shift of the transfer curve.[6,17,18] Thus, the degradation mechanism is proposed to be the drift and accumulation of the existing V_o^{2+} in the a-IGZO to the back-channel surface under the electric field.[4] As shown in Fig. 7(b), no recovery of the degradation is observed in 60 s after the stress is removed. This finding is different from the recovery behavior of NBS degradation. It is consistent with the involvement of V_o^{2+}, which is more stable than V_o^{+}.[19]

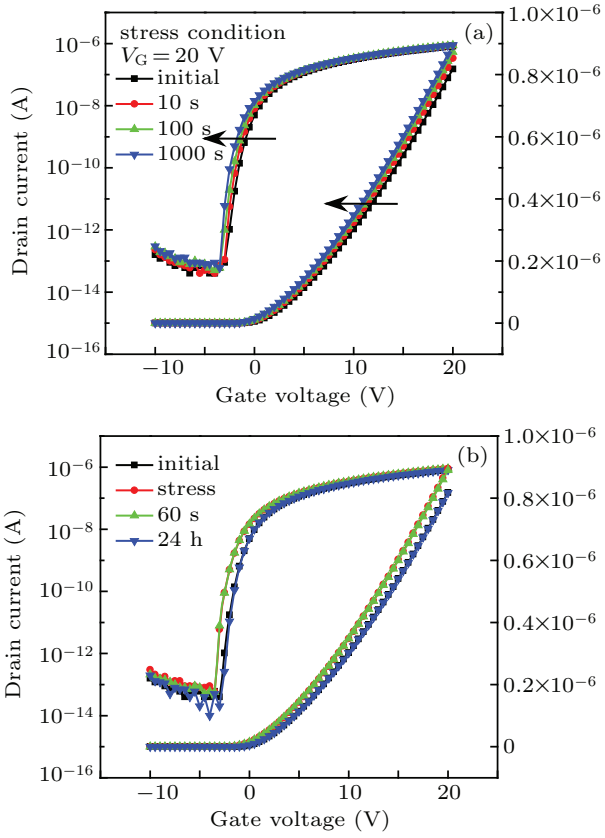


Fig. 7. Evolution of the transfer curves in linear and logarithmic scales for the TFTs (a) under PBS and (b) after PBS is removed.

However, when the a-IGZO TFT is illuminated with blue light with a power density of 2 mW/cm^2 in addition to the

PBS, it can be seen in Fig. 8(a) that the on-state current increased by 21.5% and *SS* increased from 0.47 V/decade to 0.6 V/decade after PBIS. The transfer curve in the subthreshold region further negatively shifted 0.8 V, and a decrease in the on-state current is observed after the stress is removed (Fig. 8(b)). The increase in I_{on} after PBIS is proposed to be caused by photo-generated carriers as confirmed in Fig. 5. Therefore, two degradation mechanisms are involved under PBIS. One mechanism causes degradation of *SS* and recovery in a short time; it is proposed to be the generation of V_o^+. V_o^+, as deep trap states, can trap electrons and increase the threshold voltage. The other is similar to that under PBS with V_o^{2+} accumulated at the back channel. The effects of V_o^{2+} are covered by the effects of V_o^+ immediately after PBIS, and the negative shift of the transfer curve emerges after the removal of PBIS and the recovery of the V_o^+.

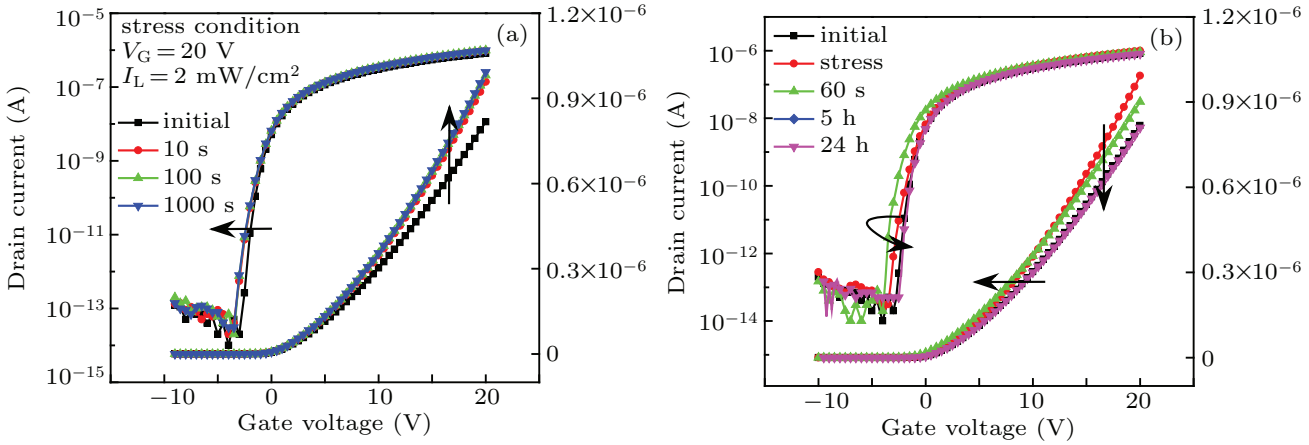


Fig. 8. Evolution of the transfer curves in linear and logarithmic scales for scales the TFTs (a) under PBIS and (b) after PBIS is removed.

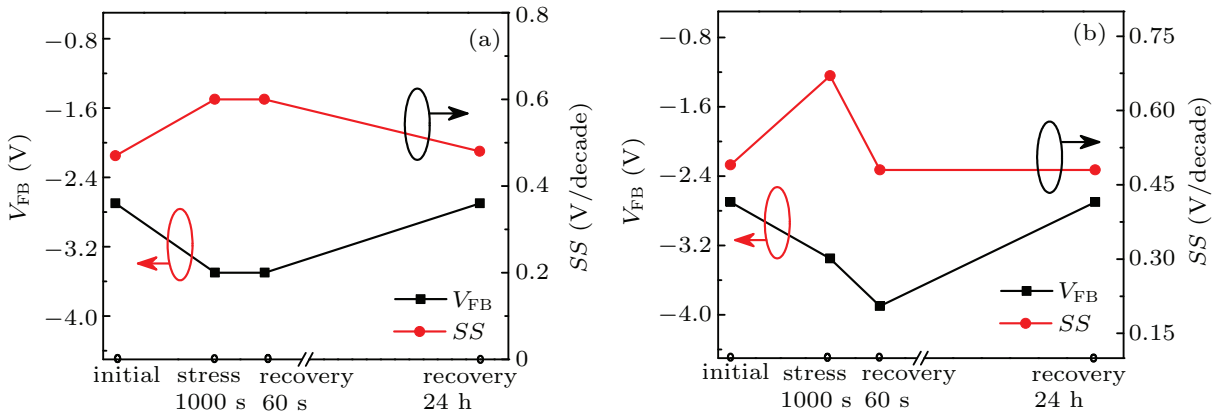


Fig. 9. V_{FB} and *SS* at the initial, after stress for 1000 s and 60 s and 24 h after the stress is removed for the cases of (a) PBS and (b) PBIS.

3.3. Degradation mechanism with V_o^+

Therefore, the introduction of V_o^+ is the dominant degradation mechanism under NBS and a small amount of V_o^+ can also be induced under PBIS. They can be explained with the band diagrams shown in Fig. 10. When a negative gate bias is applied, the energy band is bent upward, and the Fermi level is close to the valance band at the channel surface. Electrons at the trap states of neutral oxygen vacancies higher than the Fermi level are emitted, and the neutral oxygen vacancies are ionized into V_o^+ and V_o^{2+}, which are distributed as deep trap states and shallow trap states in the bandgap, respectively. V_o^+ results in the degradation of *SS* and the increase in V_{TH} and V_{FB}. The number of V_o^{2+} is relatively small, such that its effect is minimal. Moreover, V_o^+ is metastable and easy to recombine with electrons, so the degradation recovers quickly after removing the stress. It is speculated that nitrogen is introduced into the channel a-IGZO from the gate dielectric during the annealing processes for dehydrogenation and formation of source/drain. They can form Zn=N bonds with one Zn atom at an oxygen vacancy site and the other Zn atom then tends to form V_o^+ when it is ionized.[20]

When a positive gate voltage is applied after NBS, high-concentration electrons accumulate at the channel surface, and the accumulated V_o^+ can recombine with electrons more quickly. This recovery process requires only a few milliseconds.[21] Thus, when the transfer curve is measured with suf-

ficiently high positive gate voltages, the current exhibits a step-like rise and the slopes of the curves of the on-state region rises, as shown in Figs. 2 and 4. This finding can also explain the phenomenon that the degradation in the subthreshold region cannot be observed, when the transfer curve after NBS is measured with the gate voltage sweeping from positive gate bias to the negative gate bias direction, as shown in Fig. 11. This condition may also be the reason why degradation in the subthreshold swing was seldom observed and reported in the literature. For the increased V_o^+ after a longer stress time, the unrecombined V_o^+ under a positive gate bias can minimally decrease the on-state current.

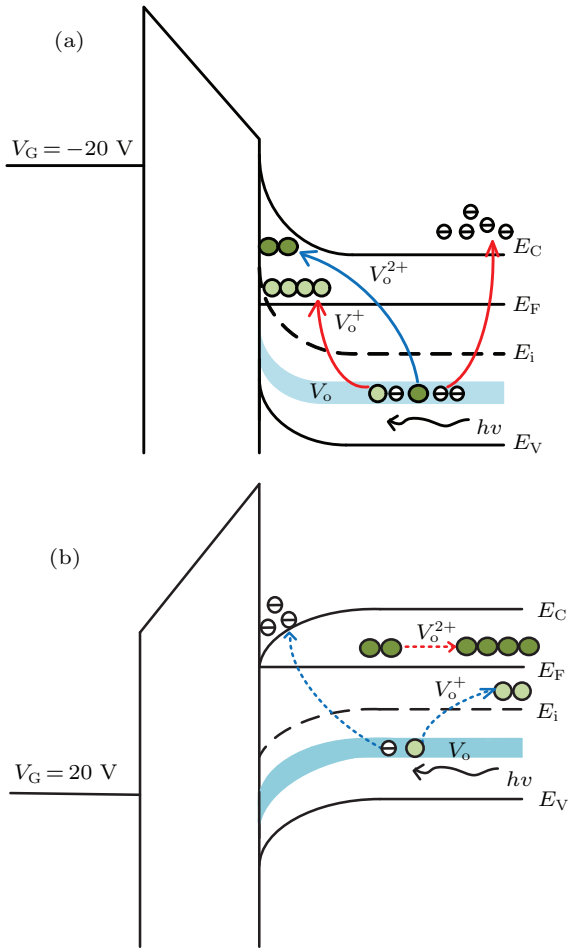


Fig. 10. Schematic energy band diagrams showing the generation of V_o^+ and V_o^{2+} under (a) NBIS and (b) PBIS.

With the help of blue light, V_o and part of V_o^+ transit to V_o^{2+}, as schematically shown in Fig. 10(a). V_o^{2+} accumulates at the channel/gate dielectric interface due to the negative gate voltage, causing a negative shift of V_{FB}. It cannot recover rapidly in seconds because the recombination speed of V_o^{2+} is slower than that of V_o^+. When these mechanisms occur simultaneously, the negative shift of V_{FB} is not apparent until the degradation in the subthreshold region is recovered. Under the coexistence of the two mechanisms, *SS* is degraded, V_{TH} is increased, but V_{FB} shows slight increase under NBIS.

When a positive gate bias is applied, the energy band is bent downward and the Fermi level is close to the conduction band minimum, the neutral oxygen vacancies remain neutral with electrons. Thus, the transfer curve after PBS only exhibits a slightly negative shift due to the accumulation of the existing V_o^{2+} in the a-IGZO at the back channel surface. When illuminated with light due to sufficiently large photon energy, a limited amount of the neutral oxygen vacancies can be ionized into V_o^+, thereby degrading the subthreshold swing and increasing the threshold voltage by the trapping electrons in the channel.

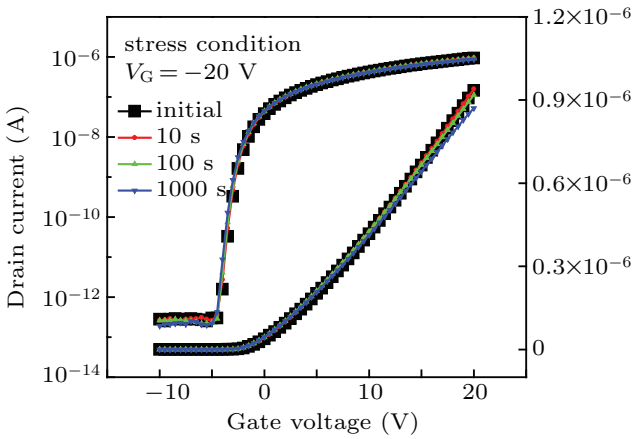


Fig. 11. Evolution of the transfer curves in linear and logarithmic scales for the TFTs under NBS measured from positive gate voltage to negative gate voltage.

3.4. Simulation verification

Silvaco ATLAS is utilized to simulate the TFT's transfer characteristics before and after stress to verify the speculations. The parameter values used for the simulation of the initial transfer curves are listed in Table 2. The simulation results are compared with the experimental data in Fig. 12. The distribution of the added trap states during the simulation of the transfer curves after 1000-s stress time for various types of stress are plotted in Fig. 13, and the parameters for the added trap states are summarized in Table 3. When deep trap states, expressed with g_{GD}, are added in the channel, the degradation phenomenon, including increased V_{FB}, V_{TH}, and *SS*, is similar to the measurement results under NBS (Fig. 12(a)). Then, the positive charge representing V_o^{2+}, described with g_{OV}, at the gate dielectric/a-IGZO interface is added, and V_{FB} becomes smaller than that after NBS, similar to the measurement results under NBIS. Figure 12(b) shows that the transfer curve is similar to the measurement results under PBS when V_o^{2+}, described with g_{OV}, at the back-channel surface is increased. With the addition of a small amount of deep level defects described with g_{GD} in the channel, *SS* and V_{TH} are further increased, similar to the measurement results under PBIS. These simulation results confirm that our speculations are reasonable.

Table 2. Parameters for the simulation of the initial transfer curves of the initial a-IGZO TFT.

Parameters	Value (Initial)	Description
N_C (cm^{-3})	5×10^{18}	effective density of states in conduction band
N_V (cm^{-3})	5×10^{18}	effective density of states in valence band
E_g (eV)	3.2	band-gap
μ_n (cm^2/V·s)	6	electron mobility
Tail acceptor-like states		$g_{TA}(E)=N_{TA}\times\exp[(E-E_C)/W_{TA}]$
N_{TA}(cm^{-3}·eV^{-1})	9×10^{19}	conduction band edge intercept densities
W_{TA} (eV)	0.035	conduction band characteristic decay energy
Tail donor-like states		$g_{TD}(E)=N_{TD}\times\exp[(E_V-E)/W_{TD}]$
N_{TD} (cm^{-3}·eV^{-1})	8×10^{19}	valence band edge intercept densities
W_{TD} (eV)	0.01	valence band characteristic decay energy
Shallow donor DOS		$g_{OV}(E)=N_{OV}\times\exp[-(E-E_{OV}/W_{OV})^2]$
N_{OV} (cm^{-3}·eV^{-1})	5×10^{17}	total density of oxygen vacancy (OV) states
E_{OV} (eV)	2.9	peak energy of OV states
W_{OV} (eV)	0.1	characteristic decay energy of OV states
Deep donor-like states		$g_{GD}(E)=N_{GD}\times\exp[-(E-E_{GD}/W_{GD})^2]$
N_{GD} (cm^{-3}·eV^{-1})	1×10^{16}	total density of deep donor-like states
E_{GD} (eV)	0.13	peak energy of deep states
δ (eV)	0.1	characteristic decay energy of deep states

Table 3. Parameters for the DOS added during the simulation of the transfer curves after stress.

Parameters	Value (NBS)	Value (NBIS)	Value (PBS)	Value (PBIS)
N_{GD} (cm^{-3}·eV^{-1})	8×10^{19}	8×10^{19}		2×10^{18}
E_{GD} (eV)	0.165	0.165		0.165
N_{OV} (cm^{-3}·eV^{-1})		1×10^{19}	5×10^{16}	5×10^{16}
E_{OV} (eV)		2.9	3	3
δ (eV)		0.1	0.4	0.4

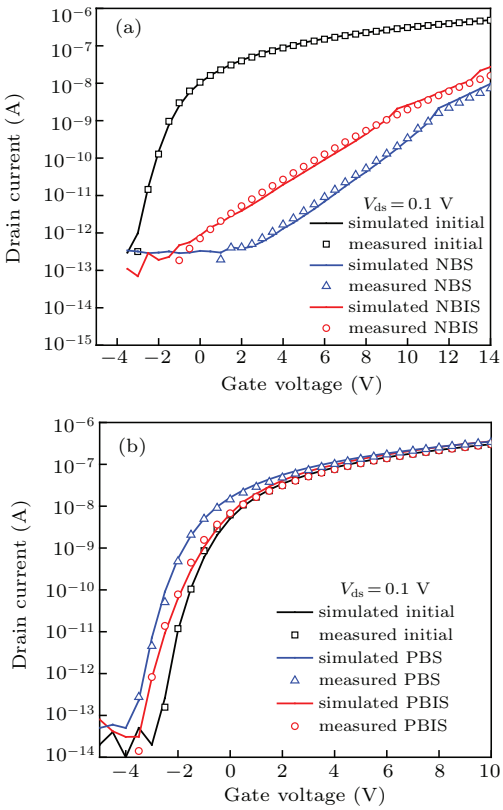


Fig. 12. Comparison of the measured and simulated transfer curves for the a-IGZO TFTs after (a) NBS and NBIS and (b) PBS and PBIS for 1000 s. The initial transfer curves are added for reference.

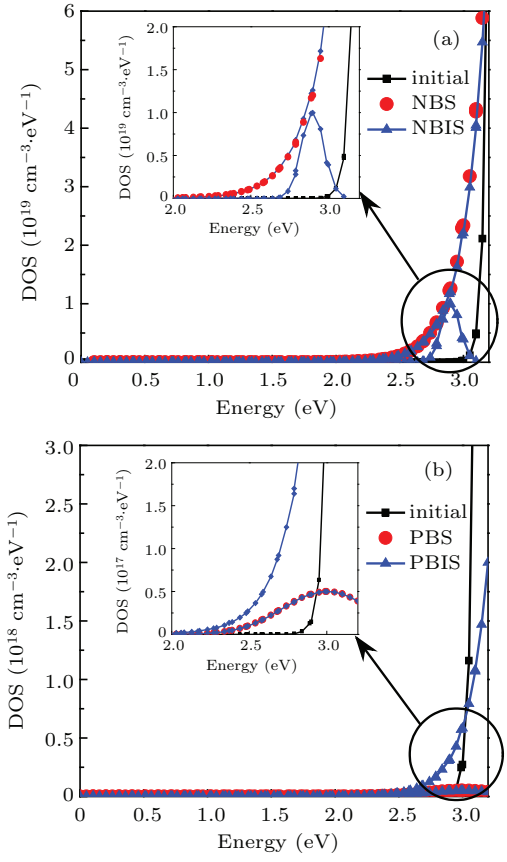


Fig. 13. Comparison of the DOS extracted after simulation for (a) the initial TFT and the TFT after NBS and NBIS for 1000 s, and (b) the initial TFT and the TFT after PBS and PBIS for 1000 s.

4. Conclusions

Increased threshold voltage and deteriorated subthreshold characteristics of a-IGZO TFTs after NBS are observed and proposed to be due to the generation of V_o^+, which is more

significant than V_o^{2+}. When illumination with blue light is applied in addition to NBS, the increase in threshold voltage is reduced given that more V_o^{2+} are generated, thereby reducing the threshold voltage. Negatively shifted transfer curves are also observed after the recovery of V_o^{+} generated during PBIS. The degradation in *SS* and V_{TH} after NBS can be recovered in a very short time because V_o^{+} forms deep level defects and can recombine with electrons quickly. In addition, the degradation phenomena cannot be observed when the transfer curves are measured from the positive gate bias to the negative gate bias direction. The generation of V_o^{+} after NBS and V_o^{+} and V_o^{2+} is successfully verified by the simulation with Silvaco ATLAS.

References

[1] Yamazaki S, Hirohashi T, Takahashi M, Adachi S, Tsubuku M, Koezuka J, Okazaki K, Kanzaki Y, Matsukizono H, Kaneko S, Mori S and Matsuo T 2014 *Journal of the Society for Information Display* **22** 55

[2] Lu L and Wang M 2015 *IEEE Trans. Electron Dev.* **62** 574

[3] Lu L, Li J, Feng Z, Kwok H and Wang M 2016 *IEEE Electron Dev. Lett.* **37** 728

[4] Yang Y, Zhang D, Wang M, Lu L and Wong M 2018 *IEEE Electron Dev. Lett.* **39** 707

[5] Chen T, Chang T C, Tsai C T, Hsieh T Y, Chen S C, Lin C S, Hung M C, Tu C H, Chang J J and Chen P L 2010 *Appl. Phys. Lett.* **97** 112104

[6] Tang L, Yu G, Lu H, Wu C, Qian H, Zhou D, Zhang R, Zheng Y and Huang X 2015 *Chin. Phys. B* **24** 088504

[7] Suresh A and Muth J F 2008 *Appl. Phys. Lett.* **92** 033502

[8] Li S, Wang M, Zhang D, Wang H and Shan Q 2019 *IEEE J. Electron Dev. Soc.* **7** 1063

[9] Gosain D P and Tanaka T 2009 *Jpn. J. Appl. Phys.* **48** 03

[10] Li J, Lu L, Chen R, Kwok H and Wong M 2018 *IEEE Trans. Electron Dev.* **65** 142

[11] Wang Y, Wang M, Zhang D and Wang H 2020 *Chin. Phys. B* **29** 118101

[12] Tai Y, Liu H, Chan P and Chiu S 2018 *IEEE Electron Dev. Lett.* **39** 696

[13] Meux A D J D, Bhoolokam A, Pourtois G, Genoe J and Heremans P 2017 *Phys. Status Solidi A* **214** 1770131

[14] Lee J M, Cho I T, Lee J H and Kwon H I 2008 *Appl. Phys. Lett.* **93** 093504

[15] Chiu C J, Shih S S, Weng W, Chang S, Hung Z D and Tsai T 2012 *IEEE Photon. Technol. Lett.* **24** 1018

[16] Huang X, Wu C, Lu H, Re H and Xu Q 2012 *Appl. Phys. Lett.* **100** 243505

[17] Lee J, Cho I, Lee J and Kwon H 2008 *Appl. Phys. Lett.* **93** 093504

[18] Qi D, Zhang D and Wang M 2017 *Chin. Phys. B* **26** 128101

[19] Janotti A and Walle C 2005 *Appl. Phys. Lett.* **87** 122102

[20] Li G, Zhan R, Yang B, Liu C, Dong C, Lee C, Wu Y, Lu P, Deng S, Shieh H D and Xu N 2016 *IEEE Trans. Electron Dev.* **63** 4309

[21] Billah M M and Jang J 2017 *IEEE Electron Dev. Lett.* **38** 477